Queensland University of Technology
Brisbane Australia

This is the author's version of a work that was submitted/accepted for publication in the following source:

Molla, M. M., Saha, S. C., Khan, M. A. I., & Hossain, M. A. (2011) Radiation effects on natural convection laminar flow from a horizontal circular cylinder. *Desalination and Water Treatment*, *30*, pp. 89-97.

This file was downloaded from: http://eprints.qut.edu.au/44113/

© Copyright 2011 Desalination Publications

Notice: *Changes introduced as a result of publishing processes such as copy-editing and formatting may not be reflected in this document. For a definitive version of this work, please refer to the published source:*

http://dx.doi.org/10.5004/dwt.2011.1870

Radiation effects on natural convection laminar flow from a horizontal circular cylinder

M. M. Molla[1], S. C. Saha[2], M. A. I. Khan[3], M. A. Hossain[4]
[1]Department of Mechanical and Manufacturing Engineering, University of Manitoba, Winnipeg, R3T 5V6, Canada. E-mail:molla@cc.umanitoba.ca
[2]School of Engineering & Physical Sciences, James Cook University, Townsville, QLD 4811, Australia
[3]Pathogen Control Engineering Institute, School of Civil Engineering, University of Leeds, Leeds LS2 9JT, UK
[4]Department of Mathematics, COMSATS Institute of Information Technology, Islama-bad, Pakistan

Abstract: The effect of radiation on natural convection flow from an isothermal circular cylinder has been investigated numerically in this study. The governing boundary layer equations of motion are transformed into a non-dimensional form and the resulting nonlinear systems of partial differential equations are reduced to convenient boundary layer equations, which are then solved numerically by two distinct efficient methods namely (i) Implicit finite difference method or the Keller-Box Method (KBM) and (ii) Straight Forward Finite Difference Method (SFFD). Numerical results are presented by velocity and temperature distribution of the fluid as well as heat transfer characteristics, namely the shearing stress and the local heat transfer rate in terms of the local skin-friction coefficient and the local Nusselt number for a wide range of surface heating parameter and radiation-conduction parameter. **Due to the effects of the radiation the skin-friction coefficients as well as the rate of heat transfer increased and consequently the momentum and thermal boundary layer thickness enhanced.**

Keywords: Natural convection; radiation-conduction interaction; Finite difference method, horizontal circular cylinder.

Nomenclature

a = Radius of the circular cylinder
C_p = Specific heat at constant pressure
C_f = Skin-friction coefficient
f = Dimensionless stream function
g = Acceleration due to gravity
Gr = Grashof number

k = Thermal conductivity
Nu = Nusselt number
Pr = Prandtl number
q_r = Radiation heat flux
q_c = Conduction heat flux
R_d = Radiation-conduction parameter or Planck number
T = Temperature of the fluid in the boundary layer
T_∞ = Temperature of the ambient fluid
T_w = Temperature at the surface
U, V = Dimensionless fluid velocities in the *x, y* directions
$\hat{u}, \hat{v}$ = Fluid velocities in the $\hat{x}$, $\hat{y}$ directions
$\hat{x}, \hat{y}$ = Axes in the direction along and normal to the surface respectively
$\boldsymbol{X, Y}$ **Dimensionless direction along and normal to the surface respectively**

Greek symbols
α_r = Rosseland mean absorption coefficient
β = Volumetric coefficient of thermal expansion
ψ = Stream function
τ_w = Wall shearing stress
ρ = Fluid density
μ = Dynamic viscosity of the fluid
ν = Kinematic viscosity of the fluid
θ = Dimensionless temperature function
θ_w = Surface heating parameter

Introduction

A medium is said to be optically dense if the mean free path of a radiation photon beam which travels through the medium is very small compared with the characteristic dimension of the medium. For an optically dense medium the radiative heat fluxes can be approximated by the Rosseland diffusion approximation [1], which has been greatly used in many radiation related studies. In the present work, the effects of thermal radiation with the Rosseland diffusion approximation on a free convection boundary layer flow from an isothermal cylinder have been investigated theoretically and numerically. The thermal radiation effects on the free convection flow are important in many engineering applications, such as in advanced types of power plants for nuclear rockets, high-speed flights, re-entry vehicles and processes involving high temperatures, and very little is known about the effects of radiation on the boundary-layer flow of radiating fluid past a body {see [2], Ch-13}.

At a high temperature the presence of thermal radiation alters the distribution of temperature in the boundary layer, which in turn affects the heat transfer at the wall. In such situation the simultaneous treatment of the convective and radiative heat transfer is necessary. Cess [3] studied the interaction of thermal radiation with free convection heat transfer along a vertical flat plate by considering absorbing, emitting and non-scattering gas. The singular perturbation technique was used to solve the set of non-linear partial differential equations.

An analytical attempt was made to understand the non-equilibrium interaction between the thermal radiation and the laminar free convection from a heated vertical plate immersed in a radiating gas by considering Prandtl number Pr = 1.0 [4]. Cheng and Ozisik [5] investigated the radiation with free convection from a vertical plate, considering an absorbing, emitting and isotropically scattering fluid. A viscous, radiating and non-similar boundary layer flow from a stagnation region and a flat plate has been investigated by Shwartz [6]. He studied the behaviour for an emitting and absorbing gas including the entire range of optical thickness, from thin to thick.

Hossain et al. [7] have analyzed the effect of radiation using the Rosseland diffusion approximation, which leads to non-similarity solution for the forced and free convection flow of an optically dense viscous incompressible fluid past a heated vertical plate with uniform free stream velocity and surface temperature. Using a group of transformations, the boundary layer equations governing the flow were reduced to local non-similarity equations validating both in the forced and free convection regimes.

Radiation effects on the natural convection flow about a truncated cone had been studied by Yih [8] following the Rosseland diffusion approximation. **Molla et al. [9-10] have investigated the radiation effect on mixed convection along a wavy surface and frustum of cone using the Rosseland diffusion approximation where the computational fluid was optically dense. Molla et al. [9-10] have found that the effects of radiation the rate of heat transfer from the wavy surface enhanced and consequently the thermal boundary layer increased.**

Natural convection flow of viscous incompressible fluid from a horizontal circular cylinder represents an important problem, which is related to numerous engineering applications such as to handle hot wire, steam pipe etc. It appears that Merkin [11-12]

was the first to present a complete solution of this problem, using the Blasius and Gortler series expansion method along with an integral method and a finite-difference scheme. The problem of free convection boundary layer flow on a cylinder of elliptic cross-section was also studied by Merkin [13]. Ingham [14] investigated the boundary layer flow on an isothermal horizontal cylinder. **Nazar et al. [15] have investigated the natural convection flow along a uniformly heated horizontal circular cylinder considering the micro polar fluid. They described the effects of micro-rotation of the fluid on the heat transfer and the skin-friction coefficient. To the best of our knowledge, radiation effects on free convection flow from an isothermal horizontal circular cylinder have not yet been studied and the present work demonstrates this issue.**

In the present study, it is proposed to investigate the natural convection flow of an optically dense viscous incompressible fluid past an isothermal horizontal circular cylinder, considering the Rosseland diffusion approximation. The basic equations of motion are transformed into convenient forms, which are solved numerically using a very efficient finite-difference scheme together with the Keller-box method ([16]) and the straight forward finite difference method. Consideration is given to the situation where the buoyancy forces assist the natural convection flow for various combinations of the radiation-conduction parameter R_{d} and the surface heating parameter θ_w. The numerical results allow us to predict the different behaviour that can be observed when the relevant parameters are varied.

Formulation of problem

A steady two-dimensional laminar free convective flow from an isothermal circular cylinder of radius a, which is immersed in a viscous and incompressible optically dense fluid, is considered. It is assumed that the surface temperature of the cylinder is T_w, where $T_w > T_\infty$. Here T_∞ is the ambient temperature of the fluid and T is the temperature of the fluid. The physical configuration considered is as shown in Figure 1.

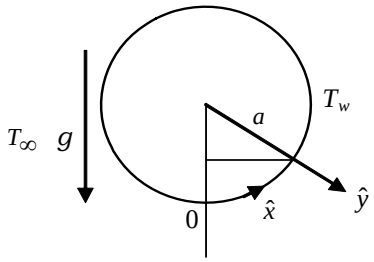

Figure 1 : Physical model and coordinate system.

Under the usual Bousinesq approximation, following Merkin [11] the equations governing the flow are

$$\frac{\partial \hat{u}}{\partial \hat{x}} + \frac{\partial \hat{v}}{\partial \hat{y}} = 0, \tag{1}$$

$$\rho\left(\hat{u}\frac{\partial \hat{u}}{\partial \hat{x}} + \hat{v}\frac{\partial \hat{u}}{\partial \hat{y}}\right) = \mu\frac{\partial^2 \hat{u}}{\partial \hat{y}^2} + \rho g\beta\left(T - T_\infty\right)\sin\left(\frac{\hat{x}}{a}\right), \tag{2}$$

$$\hat{u}\frac{\partial T}{\partial \hat{x}} + \hat{v}\frac{\partial T}{\partial \hat{y}} = \frac{k}{\rho C_p}\frac{\partial^2 T}{\partial \hat{y}^2} - \frac{1}{\rho C_p}\frac{\partial q_r}{\partial \hat{y}}, \tag{3}$$

where $(\hat{u},\hat{v})$ are the velocity components along the $(\hat{x},\hat{y})$ axes, g is the acceleration due to gravity, ρ is the fluid density, k is the thermal conductivity, β is the coefficient of thermal expansion, μ is the viscosity of the fluid, C_p is the specific heat at constant pressure, and q_r on the right hand side of equation (3) represents the radiative heat flux in the $\hat{y}$ direction.

The appropriate boundary conditions to solve equations (1)-(3) are

$$\hat{u} = \hat{v} = 0, \quad T = T_w \text{ at } \hat{y} = 0, \tag{4a}$$

$$\hat{u} \to 0, \quad T \to T_\infty \quad \text{as} \quad \hat{y} \to \infty. \tag{4b}$$

This radiation heat flux, q_r, is simplified by the Rosseland diffusion approximation as

$$q_r = -\frac{4\sigma}{3k\left(\alpha_r + \sigma_s\right)}\frac{\partial T^4}{\partial \hat{y}} \tag{5a}$$

where σ is the Stefan-Boltzmann constant, α_r is the Rosseland mean absorption coefficient and σ_s is the scattering coefficient. As it is reported by Rapits [17], the fluid-phase temperature differences within the flow are assumed sufficiently small so that T^4 may be expressed as a linear function of temperature. This is done by expanding T^4 in a

Taylor series about the free-stream temperature T_∞ and neglecting higher-order terms to give $T^4 \cong 4T_\infty^3 T - 3T_\infty^4$.

Therefore (5a) becomes

$$q_r = -\frac{14\sigma T_\infty^3}{3k(\alpha_r + \sigma_s)}\frac{\partial^2 T}{\partial \hat{y}^2} \tag{5b}$$

The limitation to the use of the Rosseland diffusion approximation should be recognized. It is valid in the interior of a medium, is not employed near the boundaries, and is good only for intensive absorption, that is, for an optically thick boundary layer. The approximation cannot provide a complete description of the physical situation near the boundaries since it does not include any terms for radiation from the boundary surface. However, the boundary surface effects are negligible in the interior of an optically thick region since the radiation from the boundaries is attenuated before reaching the interior.

We now introduce the following non-dimensional variables:

$$x = \frac{\hat{x}}{a},\ y = Gr^{1/4}\left(\frac{\hat{y}}{a}\right), \quad u = \frac{a}{\nu}Gr^{-1/2}\hat{u}, \quad v = \frac{a}{\nu}Gr^{1/4}\hat{v},$$
$$\theta = \frac{T - T_\infty}{T_w - T_\infty}, \qquad Gr = \frac{g\beta(T_w - T_\infty)a^3}{\nu^2}, \tag{6}$$

where ν (=μ/ρ) is the reference kinematic viscosity and *Gr* is the Grashof number, θ is the non-dimensional temperature function .

Substituting the variables (6) into equations (1)-(4) lead to the following non-dimensional equations

$$\frac{\partial u}{\partial x} + \frac{\partial v}{\partial y} = 0, \tag{7}$$

$$u\frac{\partial u}{\partial x} + v\frac{\partial u}{\partial y} = \frac{\partial^2 u}{\partial y^2} + \theta \sin x, \tag{8}$$

$$u\frac{\partial \theta}{\partial x} + v\frac{\partial \theta}{\partial y} = \frac{1}{\Pr}\frac{\partial}{\partial y}\left[\left\{1 + \frac{4}{3}R_d(1+\Delta\theta)^3\right\}\frac{\partial \theta}{\partial y}\right], \tag{9}$$

and the corresponding boundary conditions are

$$u = v = 0, \quad \theta = 1 \quad \text{at} \quad y = 0, \tag{10a}$$
$$u \to 0, \quad \theta \to 0 \quad \text{as} \quad y \to \infty, \tag{10b}$$

where R_d is the radiation-conduction parameter or Planck number, θ_w is the surface heating parameter and Pr is the Prandtl number, which are defined respectively as

$$R_d = \frac{4\sigma T_\infty^3}{k(\alpha_r + \sigma_s)},\ \theta_w = \frac{T_w}{T_\infty}, \Delta = \theta_w - 1 \quad \text{and} \ \ \Pr = \frac{\mu C_p}{k} \qquad . \tag{11}$$

Numerical methods

Investigating the present problem the authors have employed two numerical methods, namely, implicit finite difference Method or Keller box method (KBM) are elaborately described by Cebeci and Bradshaw [18] and the straight forward finite difference (SFFD), which are individually described below.

Implicit Finite Difference or Keller Box Method (KBM)

To solve equations (7)-(9), subject to the boundary conditions (10), we assume the following transformations

$$\psi = xf(x,y), \quad \theta = \theta(x,y), \tag{12}$$

where ψ is the non-dimensional stream function defined in the usual way as

$$u = \frac{\partial \psi}{\partial y}, \quad v = -\frac{\partial \psi}{\partial x}. \tag{13}$$

Substituting (13) into equations (7)-(10) and after some algebraic manipulations, the transformed equations take the following form

$$\frac{\partial^3 f}{\partial y^3} + f\frac{\partial^2 f}{\partial y^2} - \left(\frac{\partial f}{\partial y}\right)^2 + \frac{\sin x}{x}\theta = x\left(\frac{\partial f}{\partial y}\frac{\partial^2 f}{\partial x \partial y} - \frac{\partial f}{\partial x}\frac{\partial^2 f}{\partial y^2}\right), \tag{14}$$

$$\frac{1}{\Pr}\frac{\partial}{\partial y}\left[\left\{1 + \frac{4}{3}R_d\left(1 + (\theta_w - 1)\theta\right)^3\right\}\frac{\partial \theta}{\partial y}\right] + f\frac{\partial \theta}{\partial y} = x\left(\frac{\partial f}{\partial y}\frac{\partial \theta}{\partial x} - \frac{\partial \theta}{\partial y}\frac{\partial f}{\partial x}\right), \tag{15}$$

along with the boundary conditions

$$f = \frac{\partial f}{\partial y} = 0, \quad \theta = 1 \qquad \text{at} \quad y = 0, \tag{16a}$$

$$\frac{\partial f}{\partial y} \to 0, \quad \theta \to 0 \quad \text{as} \quad y \to \infty. \tag{16b}$$

It can be seen that near the lower stagnation point of the cylinder i.e. when $x \approx 0$, equations (14) and (15) reduce to the following ordinary differential equations

$$f''' + ff'' - f'^2 + \theta = 0, \tag{17}$$

$$\frac{1}{\Pr}\left[\left\{1 + \frac{4}{3}R_d\left(1 + (\theta_w - 1)\theta\right)^3\right\}\theta'\right]' + f\theta' = 0, \tag{18}$$

subject to the boundary conditions,

$$f(0) = f'(0) = 0, \quad \theta(0) = 1, \tag{19a}$$

$$f' \to 0, \quad \theta \to 0 \quad \text{as} \quad y \to \infty. \tag{19b}$$

In the above equations primes denote differentiation with respect to y.

The physical quantities of principle interest are the shearing stress and the rate of heat transfer in terms of the skin-friction coefficient C_f and the Nusselt number Nu respectively, which can be written as

$$C_f = \frac{(\tau_w)_{\hat{y}=0}}{\rho U_\infty^2} \text{ and } \quad Nu = \frac{a(q_c + q_r)_{\hat{y}=0}}{k(T_w - T_\infty)}, \tag{20}$$

$$\text{where } \quad \tau_w = \mu\left(\frac{\partial \hat{u}}{\partial \hat{y}}\right) \text{and } \quad q_c = -k\left(\frac{\partial T}{\partial \hat{y}}\right). \tag{21}$$

Using the variables (5), (6), (13) and the boundary condition (16a) into equations (20)-(21), we get

$$C_f Gr^{1/4} = x\frac{\partial^2 f(x,0)}{\partial y^2}, \tag{22}$$

$$NuGr^{-1/4} = -\left(1 + \frac{4}{3}R_d\theta_w^3\right)\frac{\partial \theta(x,0)}{\partial y}. \tag{23}$$

The results of the velocity and temperature distributions are calculated respectively from the following relations

$$u = x\frac{\partial f}{\partial y}, \quad \theta = \theta(x, y). \tag{24}$$

A very efficient and accurate implicit finite difference method (the Keller box method) is employed to solve the nonlinear system of partial differential equations (14)-(15). The equations (14)-(15) are written in terms of first order equations in y, which are then expressed in finite difference form by approximating the functions and their derivatives in terms of the central differences in both coordinate directions. Denoting the mesh points in the (x, y) plane by x_i and y_j, where i = 1, 2, 3, …, M and j = 1, 2, 3, …, N, central difference approximations are made such that the equations involving x explicitly are centred at $(x_{i-1/2}, y_{j-1/2})$ and the remainder at $(x_i, y_{j-1/2})$, where $y_{j-1/2} = (y_j + y_{j-1})/2$, etc. This results in a set of nonlinear difference equations for the unknowns at x_i in terms of their values at x_{i-1}. These equations are then linearised by the Newton's quasi-linearization technique and are solved using a block-tridiagonal algorithm, taking as the initial iteration of the converged solution at $x = x_{i-1}$. Now to initiate the process at x = 0, we first provide guess profiles for all five variables (arising the reduction to the first order form) and use the Keller box method to solve the governing ordinary differential equations. Having obtained the lower stagnation point solution it is possible to march step by step

along the boundary layer. For a given value of *x*, the iterative procedure is stopped when the difference in computing the velocity and the temperature in the next iteration is less than 10^{-5}, i.e. when $|\delta f^{i}| \leq 10^{-5}$, where the superscript denotes the iteration number.

Straight forward finite difference (SFFD)

The new transformations for the SFFD

$$X = x, \quad Y = y, \quad U = \frac{u}{x}, \quad V = v, \tag{25}$$

Using (25) into (7)-(10), yields

$$X\frac{\partial U}{\partial X} + U + \frac{\partial V}{\partial Y} = 0, \tag{26}$$

$$XU\frac{\partial U}{\partial X} + V\frac{\partial U}{\partial Y} + U^{2} = \frac{\partial^{2} U}{\partial Y^{2}} + \theta\frac{\sin X}{X}, \tag{27}$$

$$XU\frac{\partial \theta}{\partial X} + V\frac{\partial \theta}{\partial Y} = \frac{1}{\Pr}\frac{\partial}{\partial Y}\left[\left\{1 + \frac{4}{3}R_{d}\left(1 + (\theta_{w} - 1)\theta\right)^{3}\right\}\frac{\partial \theta}{\partial Y}\right]. \tag{28}$$

The corresponding boundary conditions are

$$U = V = 0, \quad \theta = 1 \quad \text{at} \quad X = 0 \quad \text{any} \quad Y, \tag{29a}$$

$$U = V = 0, \quad \theta = 1 \quad \text{at} \quad Y = 0, \quad X > 0, \tag{29b}$$

$$U \to 0, \quad \theta \to 0 \quad \text{as} \quad Y \to \infty, \quad X > 0. \tag{29c}$$

Now equations (26)-(28) subject to the boundary conditions (29) are discretised using the central-difference for diffusion terms and the forward-difference for the convection terms, finally we get a system of tri-diagonal algebraic equations. The algebraic equations have been solved by double sweep technique. The numerical discretisation of the equations (26)-(28) are given below:

$$V_{i,j} = V_{i,j-1} - \Delta Y\frac{1}{2}\left(U_{i,j-1} + U_{i,j}\right) - X_{i}\frac{\Delta Y}{\Delta X}\left(U_{i,j} - U_{i-1,j}\right), \quad j = 2\ldots N, i = 1\ldots M. \tag{30}$$

The momentum equation

$$X_{i}U_{i}\left(\frac{U_{i,j} - U_{i-1,j}}{\Delta X}\right) + V_{i,j}\left(\frac{U_{i,j+1} - U_{i,j-1}}{2\Delta Y}\right) + U_{i,j}^{2} = \left(\frac{U_{i,j+1} - 2U_{i,j} + U_{i,j-1}}{\Delta Y^{2}}\right) + \frac{\theta_{i,j}\sin X_{i}}{X_{i}} \tag{31}$$

And the energy equation

$$X_i U_i \left(\frac{\theta_{i,j} - \theta_{i-1,j}}{\Delta X} \right) + V_{i,j} \left(\frac{\theta_{i,j+1} - \theta_{i,j-1}}{2\Delta Y} \right) = \frac{1}{\Pr} \frac{\partial}{\partial Y} \left[\left\{ 1 + \frac{4}{3} R_d \left(1 + (\theta_w - 1)\theta_{i,j} \right)^3 \right\} \left(\frac{\theta_{i,j+1} - \theta_{i,j-1}}{2\Delta Y} \right) \right] \tag{32}$$

where N and M are the maximum numbers of Y and X-points respectively.

The computation is started from $X = 0.0$, and then marches up to the upper stagnation point of the circular cylinder ($X \approx \pi$). Here $\Delta x = \pi/180$ and $\Delta y = 0.01$ are used for the X- and Y- grids respectively. Now it can be calculated the skin-friction coefficient and the rate of heat-transfer from the following dimensionless relations:

$$C_f Gr^{1/4} = X \left(\frac{\partial U}{\partial Y} \right)_{Y=0}, \tag{33}$$

$$NuGr^{-1/4} = -\left(1 + \frac{4}{3} R_d \theta_w^3 \right) \left(\frac{\partial \theta}{\partial Y} \right)_{Y=0}. \tag{34}$$

Results and discussion

The numerical results for the skin-friction coefficient $C_f Gr^{1/4}$ and the Nusselt number $NuGr^{-1/4}$ are obtained for representative values of the radiation-conduction parameter R_d (= 0.0, 0.2, 0.5, 0.8, 1.0) and surface heating parameter θ_w (=1.1, 1.3, 1.6, 1.9) against the curvature parameter $x \in [0, \pi]$. It should be noted that for both CO_2 in the temperature range of 37.78-343° C (with the corresponding Prandtl number range 0.76-0.6) and NH_3 vapour in the temperature range of 48.9-204° C (with the corresponding Prandtl number 0.88-0.84) the value of R_d at 1 atm ranges from 0.033 to 0.1, whereas for water vapour in the temperature range of 104-482° C (with the corresponding Prandtl number Pr ≈ 1.0), the R_d values lie between 0.02 and 0.3 (see [3]). **It should be noted that without radiation effect ($R_d = 0.0$), we recover the problem that discussed by Merkin [11] and Nazar et al. [15] considering Pr = 1.0 which is shown in Table I.**

Table I. Comparison of the present numerical values of $C_f Gr^{1/4}$ and $NuGr^{-1/4}$ with those of Merkin [11] and Nazar et al. [15] while Pr = 1.0 and $R_d = 0.0$.

$C_f Gr^{1/4}$	$NuGr^{-1/4}$

X	Mer-kin [11]	Nazar et al. [15]	Present results by KBM	Present results by SFFD	Merkin [11]	Nazar et al. [15]	Present results by KBM	Present results by SFFD
0.0	**0.0000**	**0.0000**	**0.0000**	**0.0000**	**0.4214**	**0.4214**	**0.4216**	**0.4214**
$\pi/6$	**0.4151**	**0.4148**	**0.4139**	**0.4149**	**0.4161**	**0.4161**	**0.4163**	**0.4166**
$\pi/3$	**0.7558**	**0.7542**	**0.7527**	**0.7553**	**0.4007**	**0.4005**	**0.4006**	**0.4015**
$\pi/2$	**0.9579**	**0.9545**	**0.9526**	**0.9572**	**0.3745**	**0.3741**	**0.3741**	**0.3753**
$2\pi/3$	**0.9756**	**0.9698**	**0.9677**	**0.9347**	**0.3364**	**0.3355**	**0.3355**	**0.3210**
$5\pi/6$	**0.7822**	**0.7740**	**0.7717**	**0.7811**	**0.2825**	**0.2811**	**0.2810**	**0.2827**
π	**0.3391**	**0.3265**	**0.3238**	**0.3359**	**0.1945**	**0.1916**	**0.1911**	**0.1934**

The numerical results of the skin-friction coefficient $C_fGr^{1/4}$ and the Nusselt number $NuGr^{-1/4}$ for different values of the radiation-conduction parameter R_d (= 0.0, 1.0, 2.0, 3.0) while θ_w = 1.1 and Pr = 0.73 are illustrated in Figures. 2(a)-(b) respectively. Here we notice that the agreement between the results obtained by using the KBM and the SFFD is excellent indeed. From the figures, it can be seen that an increase in radiation-conduction parameter R_d leads to an increase in the skin-friction coefficient $C_fGr^{1/4}$ and the Nusselt number $NuGr^{-1/4}$. This may be attributed to the fact that the increase of the values of R_d implies more interaction of radiation with momentum and thermal boundary layers.

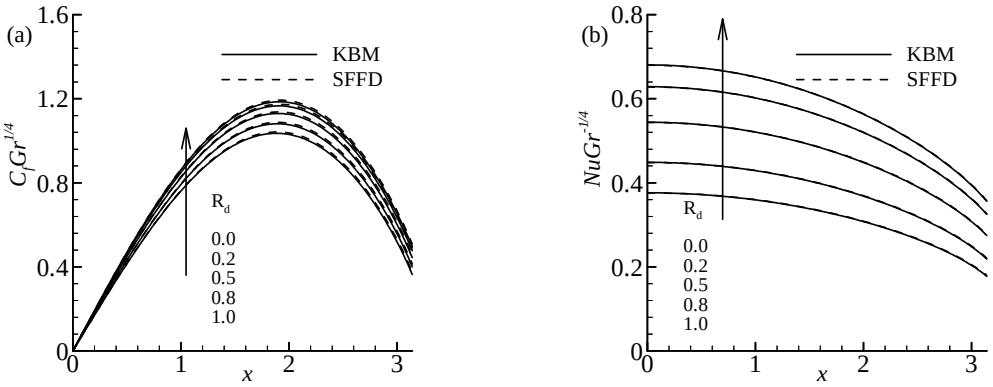

Figure 2: (a) Skin-friction, (b) Rate of heat transfer for different values of R_d while θ_w = 1.1 and Pr = 0.73

In Tables II and III, the results of the skin-friction coefficient $C_fGr^{1/4}$ and the Nusselt number $NuGr^{-1/4}$ are shown respectively for different values of surface heating parameter θ_w (=1.1, 1.3, 1.6, 1.9), while R_d = 0.5 and Pr =0.73. Again the comparisons

between the two solutions of KBM and SFFD method are found to be in excellent agreement. We further notice that an increase in the values of the surface heating parameter θ_w leads to an enhancement in the results of $C_fGr^{1/4}$ and $NuGr^{-1/4}$. For example, at $x = \pi/2$, the skin-friction coefficients $C_fGr^{1/4}$ and $NuGr^{-1/4}$ increase by 11.28% and 59.87% respectively while θ_w increases from 1.1 to 1.9. This phenomenon can easily be understood from the fact that when the surface heating parameter θ_w increases, the temperature of the surface rises and the thickness of the thermal boundary layer grows. Therefore, the surface rate of heat transfer, that is the Nusselt number $NuGr^{-1/4}$, increases. Again, this temperature increase of the fluid corresponds to the high surface shear stress which augments the skin-friction coefficient $C_fGr^{1/4}$.

Table II: The results of $C_fGr^{1/4}$ for different values of surface heating parameter θ_w while $R_d = 0.5$ and Pr = 0.73.

x	$C_fGr^{1/4}$							
	$\theta_w = 1.1$		$\theta_w = 1.3$		$\theta_w = 1.6$		$\theta_w = 1.9$	
	KBM	SFFD	KBM	SFFD	KBM	SFFD	KBM	SFFD
0.0	0.00000	0.00000	0.00000	0.00000	0.00000	0.00000	0.00000	0.00000
$\pi/6$	0.46890	0.47001	0.48173	0.48288	0.50112	0.50230	0.51907	0.52023
$\pi/3$	0.85457	0.85760	0.87829	0.88147	0.91417	0.91759	0.94749	0.95110
$\pi/2$	1.08646	1.09200	1.11757	1.12339	1.16483	1.17114	1.20901	1.21582
$2\pi/3$	1.11449	1.12277	1.14851	1.15712	1.20067	1.20990	1.25008	1.25993
$5\pi/6$	0.91093	0.92186	0.94301	0.95425	0.99318	1.00498	1.04183	1.05431
π	0.44387	0.45726	0.47050	0.48412	0.51398	0.52804	0.55827	0.57293

Table III: The results of $NuGr^{-1/4}$ for different values of surface heating parameter θ_w while $R_d = 0.5$ and Pr = 0.73.

x	$NuGr^{-1/4}$							
	$\theta_w = 1.1$		$\theta_w = 1.3$		$\theta_w = 1.6$		$\theta_w = 1.9$	
	KBM	SFFD	KBM	SFFD	KBM	SFFD	KBM	SFFD
0.0	0.54424	0.54365	0.60700	0.60629	0.72160	0.72079	0.85813	0.85724
$\pi/6$	0.53776	0.53765	0.60030	0.59963	0.71478	0.71291	0.85122	0.84783
$\pi/3$	0.51845	0.51871	0.57916	0.57860	0.69082	0.68815	0.82439	0.81869
$\pi/2$	0.48591	0.48645	0.54333	0.54289	0.64942	0.64616	0.77683	0.76934
$2\pi/3$	0.43887	0.43974	0.49095	0.49128	0.58728	0.58573	0.70305	0.69850
$5\pi/6$	0.37391	0.37508	0.41936	0.42015	0.50372	0.50299	0.60565	0.60220
π	0.27466	0.27629	0.31177	0.31301	0.38160	0.38116	0.46694	0.46348

Attention is now given to the effects of pertinent parameters on the dimensionless velocity and temperature in the flow field, computed only by the KBM, and these are presented graphically in Figure 3. Figures 3(a)-(b) illustrate the velocity and temperature distributions against y for different values of the radiation-conduction parameter R_d (= 0.0, 0.2, 0.5, 0.8, 1.0) at $x = \pi/3$ while Pr = 0.73 and θ_w =1.1. These figures display how R_d influences on the fluid velocity and temperature. As R_d increases, the velocity and temperature gradients at the surface increase which again enhances the fluid velocity and temperature.

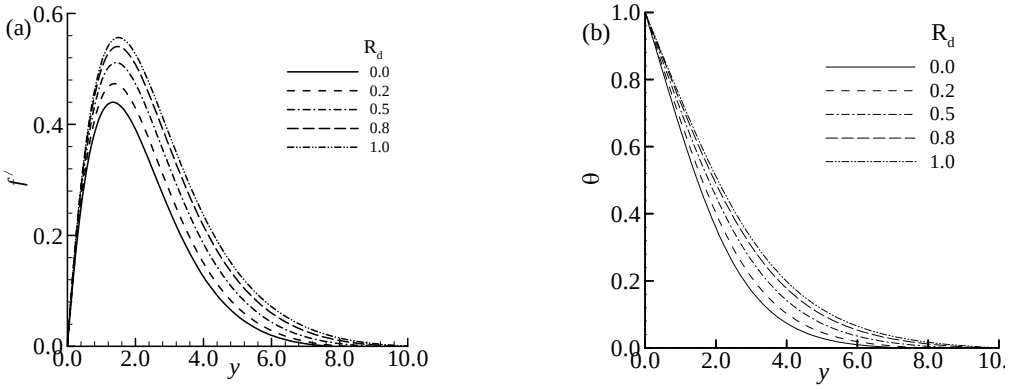

Figure 3: (a) Velocity and (b) Temperature distribution for different R_d while θ_w =1.1 and Pr = 0.73 at $x = \pi/3$.

Figures 4 and 5 illustrate the effect of the radiation-conduction parameter R_d on the development of streamlines and isotherms, which are plotted for Pr = 0.73 and θ_w = 1.1. From Figure 4(a), it is seen that without the effect of radiation (i.e. R_d = 0.0) the non-dimensional value of ψ_{max} within the computational domain is about 2.75 near the downstream point ($x \approx \pi$) of the cylinder and when the boundary layer thickness is the lowest, but ψ_{max} increases with the increment of R_d and it attains about 4.20 for R_d = 1.0 (see Figure 4(c)). This phenomenon fully coincides with the early discussion made on Figure 3(a), **the fluid speeds up** as R_d increases and the thickness of the velocity boundary layer also increases. The isotherm patterns for corresponding values of R_d are shown in Figure 5. From these three frames, we can see that the growth of thermal boundary layer over the surface of the cylinder is significant. As x increases from the lower stagnation point ($x \approx 0.0$), the hot fluid rises due to the gravity, hence the thickness of the thermal boundary layer, y, increases. This phenomenon is very straightforward as

can be seen in this frame for R_d = 1.0 in 5(c). In this case the fluid temperature increases slightly which was also noticed in Figure 3(b).

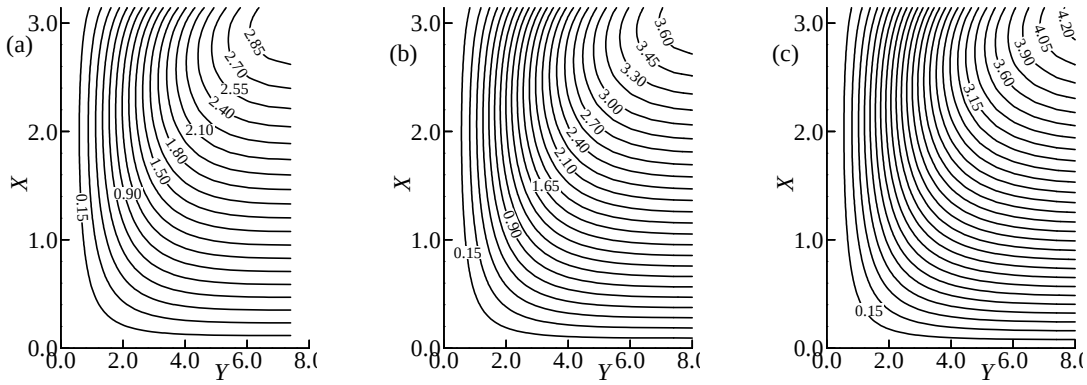

Figure 4: Streamlines for (a) R_d = 0.0 (b) R_d = 0.5 (c) R_d = 1.0 while θ_w =1.1 and Pr = 0.73

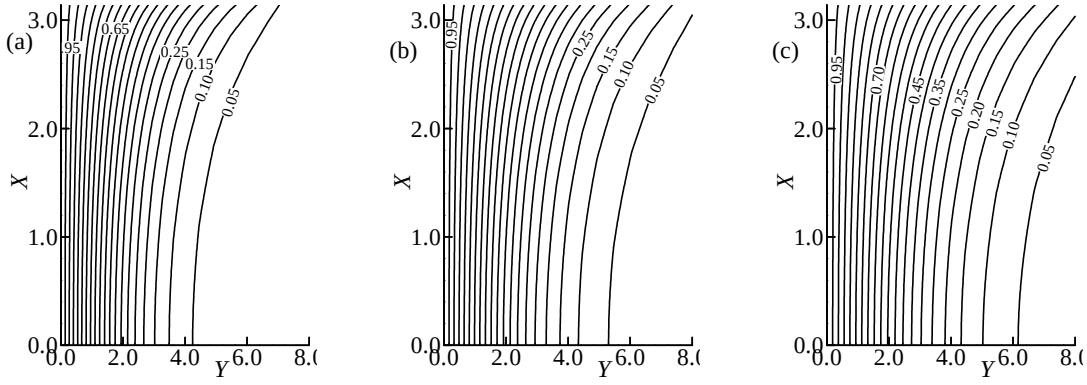

Figure 5: Isotherms for (a) R_d = 0.0 (b) R_d = 0.5 (c) R_d = 1.0 while θ_w =1.1 and Pr = 0.73

Conclusion

The effect of radiation on natural convection flow from an isothermal circular cylinder has been investigated numerically. The governing boundary layer equations of motion are transformed into a non-dimensional form and the resulting nonlinear systems of partial differential equations are reduced to convenient boundary layer equations, which are then solved numerically by two distinct efficient methods namely (i) Implicit Finite Difference Method or the Keller-box method and (ii) Straight Forward Finite Difference Method (SFFD). From the present investigation the following conclusions may be drawn:

- The skin-friction coefficient and the Nusselt number increase when the value of the radiation-conduction parameter R_d increases.
- As R_d increases, both the velocity and the temperature distribution increase significantly at $x = \pi/3$ of the surface.
- An increase in the values of θ_w leads to an increase in the values of the skin-friction coefficients and the Nusselt number.
- For increase values of R_d, the momentum and thermal boundary layer increase significantly.

References

[1] Rosseland, S. (1936), "Theoretical Astrophysics, Oxford University Press", London.

[2] Ozisik, M.N. (1973) "Radiative Transfer and Interactions with Conduction and Convection", *John Wiley & Sons*, USA.

[3] Cess, R.D. (1966), "The interaction of thermal radiation with free convection heat transfer", *Int. J. Heat Mass Transfer*, Vol. 9, pp. 1269-77.

[4] Arpaci, V.S. (1968), "Effect of thermal radiation on the laminar free convection from a heated vertical plate", *Int. J. Heat Mass Transfer*, Vol. 11, pp. 871-81.

[5] Cheng, E.H. and Ozisic, M.N. (1972), "Radiation with free convection in an absorbing, emitting and scattering medium", *Int. J. Heat Mass Transfer*, Vol.15 pp. 1243-52.

[6] Shwartz, J. (1968) "Radiation coupled viscous flows", *Int. J. Heat Mass Transfer*, Vol. 11, pp. 689-697.

[7] Hossain, M.A., Alim, M.A. and Rees, D.A.S. (1998), "Effect of thermal radiation on natural convection over cylinders of elliptic cross section", *Acta Mechanica*, Vol. 129, pp. 177-86.

[8] Yih, K.A. (1999) "Effect of radiation on natural convection about a truncated cone", *Int. J. Heat and Mass Transfer*, Vol. 42, pp. 4299-05.

[9] Molla, M.M. and Hossain, M.A. (2007), "Radiation effect on mixed convection flow along a vertical wavy surface", *Int. J. Thermal Scienc*e, Vol 46 pp. 926-935.

[10] Molla, M.M., Hossain, M.A. and Gorla, R. S. R (2009), "Radiation effect on natural convection boundary layer flow over a vertical wavy frustum of cone", *Proc. IMechE, Part C: J. Mechanical Engineering Scienc*e, Vol 223 pp. 1605-1614.

[11] Merkin J.H. (1976), Free convection boundary layer on an isothermal horizontal circular cylinders, ASME/AIChE, Heat Transfer Conference, St. Louis, Mo., August 9-11

[12] Merkin, J.H. (1977), "Mixed convection a horizontal circular cylinder", *Int. J. Heat Mass Transfer*, Vol. 20, pp. 73-77.

[13] Merkin, J.H. (1977), "Free convection boundary layer on cylinders of elliptic cross-section", *ASME, J. Heat Transfer*, Vol. 99, pp. 453-57.

[14] Ingham, D.B. (1978), "Free convection boundary layer on an isothermal horizontal cylinder", *Z. Angew. Math. Phys*., Vol. 29, pp.871-83.

[15] Nazar R., Amin N., Pop I. (2002), Free convection boundary layer on an isothermal horizontal circular cylinder in a micropolar fluid, Heat Transfer, Proceeding of the Twelfth International Conference.

[16] Keller, H.B. (1978), "Numerical methods in boundary layer theory", *Annual Rev. Fluid Mech.*, Vol. 10, pp. 417-33.

[17] Raptis, A. (1998), Flow of a micropolar fluid past a continuously moving plate by the presence of radiation, International Journal of Heat Mass Transfer, Vol. 41, pp. 2865-2866.

[18] Cebeci, T. and Bradshaw, P. (1984), "Physical and Computational Aspects of Convective Heat Transfer", *Springer, New York.*